

Topics in Mining, Metallurgy and Materials Engineering  
*Series Editor: Carlos P. Bergmann*

Stefan Johann Rupitsch

# Piezoelectric Sensors and Actuators

Fundamentals and Applications

 Springer

# **Topics in Mining, Metallurgy and Materials Engineering**

**Series editor**

Carlos P. Bergmann, Porto Alegre, Brazil

“Topics in Mining, Metallurgy and Materials Engineering” welcomes manuscripts in these three main focus areas: Extractive Metallurgy/Mineral Technology; Manufacturing Processes, and Materials Science and Technology. Manuscripts should present scientific solutions for technological problems. The three focus areas have a vertically lined multidisciplinary, starting from mineral assets, their extraction and processing, their transformation into materials useful for the society, and their interaction with the environment.

More information about this series at <http://www.springer.com/series/11054>

Stefan Johann Rupitsch

# Piezoelectric Sensors and Actuators

Fundamentals and Applications

 Springer

Stefan Johann Rupitsch  
Lehrstuhl für Sensorik  
Friedrich-Alexander-Universität  
Erlangen-Nürnberg  
Erlangen  
Germany

ISSN 2364-3293                      ISSN 2364-3307 (electronic)  
Topics in Mining, Metallurgy and Materials Engineering  
ISBN 978-3-662-57532-1              ISBN 978-3-662-57534-5 (eBook)  
<https://doi.org/10.1007/978-3-662-57534-5>

Library of Congress Control Number: 2018942913

© Springer-Verlag GmbH Germany, part of Springer Nature 2019

This work is subject to copyright. All rights are reserved by the Publisher, whether the whole or part of the material is concerned, specifically the rights of translation, reprinting, reuse of illustrations, recitation, broadcasting, reproduction on microfilms or in any other physical way, and transmission or information storage and retrieval, electronic adaptation, computer software, or by similar or dissimilar methodology now known or hereafter developed.

The use of general descriptive names, registered names, trademarks, service marks, etc. in this publication does not imply, even in the absence of a specific statement, that such names are exempt from the relevant protective laws and regulations and therefore free for general use.

The publisher, the authors and the editors are safe to assume that the advice and information in this book are believed to be true and accurate at the date of publication. Neither the publisher nor the authors or the editors give a warranty, express or implied, with respect to the material contained herein or for any errors or omissions that may have been made. The publisher remains neutral with regard to jurisdictional claims in published maps and institutional affiliations.

Printed on acid-free paper

This Springer imprint is published by the registered company Springer-Verlag GmbH, DE part of Springer Nature

The registered company address is: Heidelberger Platz 3, 14197 Berlin, Germany

# Preface

Piezoelectric devices play a major role in our everyday lives. The reason for this lies in the fact that piezoelectric materials enable an efficient conversion from mechanical energy into electrical energy and vice versa. Piezoelectric sensors and actuators represent an important subgroup of piezoelectric devices. Nowadays, the application areas of piezoelectric sensors and actuators range from process measurement technology and nondestructive testing to medicine and consumer electronics.

This book addresses students, researchers as well as industry professionals in the fields of engineering sciences, material sciences, and physics. The author aims at providing information that is important to obtain a deep understanding of piezoelectric sensors and actuators. The book additionally contains selected applications and recent developments (e.g., simulation-based material characterization), which are of great interest to science and industry.

At the beginning, we will study fundamentals of piezoelectric sensors and actuators. The fundamentals include physical basics, the principle of the piezoelectric effect and piezoelectric materials. One focus of the book relates to reliable characterization of sensor and actuator materials by combining numerical simulations with appropriate measurements. Moreover, an efficient phenomenological modeling approach for the large-signal behavior of ferroelectric materials will be presented which facilitates the operation of piezoelectric actuators. A further focus lies on piezoelectric ultrasonic transducers because they are most commonly used in applications like ultrasonic imaging and parking sensors. In this context, a nonre-active measurement approach will be detailed that allows sound field characterization in various media.

The book also deals with piezoelectric sensors and transducers in the large application area of process measurement technology. For example, we will discuss conventional piezoelectric sensors for mechanical quantities (e.g., force) as well as sensor devices for fluid flow measurements. The final part of the book concentrates on piezoelectric positioning systems and motors.

Erlangen, Germany

Stefan Johann Rupitsch

# Acknowledgements

This book was written in the course of my habilitation procedure at the Chair of Sensor Technology at the Friedrich-Alexander-University Erlangen-Nuremberg. First of all, I would like to thank Prof. Dr.-Ing. Reinhard Lerch for his valuable support and advice. He has animated me to write the book and has given me the possibility for this time-consuming activity. Moreover, I would like to thank Prof. Dr.-Ing. habil. Paul Steinmann and Prof. Dr.-Ing. habil. Jörg Wallaschek, who served as further members of the mentorship during my habilitation procedure.

I wish to express my gratitude to all the people who have inspired and sustained this work. A special thank goes to the present and former colleagues from the Chair of Sensor Technology. Many topics of the book result from cooperations with these colleagues. The dynamic and stimulating atmosphere at the Chair of Sensor Technology was certainly essential for the preparation of the book. In particular, I would like to thank (in alphabetical order) Dr.-Ing. Lizhuo Chen, Philipp Dorsch, Michael Fink, Dominik Gedeon, Florian Hubert, Dr.-Ing. Jürgen Ilg, Daniel Kiefer, Michael Löffler, Michael Nierla, Dr.-Ing. Peter Ploß, Michael Ponschab, Dr.-Ing. Thomas Scharrer, Prof. Dr.-Ing. Alexander Sutor, Manuel Weiß, Dr.-Ing. Felix Wolf, and Michael Wüst.

I also would like to thank Christine Peter for creating several drawings of the book. I gratefully acknowledge the team of the Springer-Verlag for the excellent cooperation as well as for typesetting and reading the book very carefully.

Finally, I would like to thank my girlfriend Angelina, my parents Rosmarie and Johann and my sister Barbara for their support and understanding all the time.

June 2018

Stefan Johann Rupitsch

# Contents

<b>1</b>	<b>Introduction</b>	1
1.1	Fundamentals of Sensors and Actuators	1
1.2	History of Piezoelectricity and Piezoelectric Materials	2
1.3	Practical Applications of Piezoelectricity	3
1.4	Chapter Overview	4
<b>2</b>	<b>Physical Basics</b>	7
2.1	Electromagnetics	7
2.1.1	Maxwell's Equations	7
2.1.2	Electrostatic Field	9
2.1.3	Interface Conditions for Electric Field	10
2.1.4	Lumped Circuit Elements	12
2.2	Continuum Mechanics	15
2.2.1	Navier's Equation	15
2.2.2	Mechanical Strain	18
2.2.3	Constitutive Equations and Material Behavior	21
2.2.4	Elastic Waves in Solids	23
2.3	Acoustics	26
2.3.1	Fundamental Quantities	27
2.3.2	Wave Theory of Sound	28
2.3.3	Linear Acoustic Wave Equation	33
2.3.4	Reflection and Refraction of Sound	35
2.3.5	Sound Absorption	38
	References	40
<b>3</b>	<b>Piezoelectricity</b>	43
3.1	Principle of Piezoelectric Effect	43
3.2	Thermodynamical Considerations	45
3.3	Material Law for Linear Piezoelectricity	49
3.4	Classification of Electromechanical Coupling	53

3.4.1	Intrinsic Effects . . . . .	53
3.4.2	Extrinsic Effects . . . . .	54
3.4.3	Modes of Piezoelectric Effect . . . . .	55
3.5	Electromechanical Coupling Factors . . . . .	57
3.5.1	Conversion from Mechanical into Electrical Energy . . . . .	58
3.5.2	Conversion from Electrical into Mechanical Energy . . . . .	60
3.6	Piezoelectric Materials . . . . .	63
3.6.1	Single Crystals . . . . .	64
3.6.2	Polycrystalline Ceramic Materials . . . . .	69
3.6.3	Polymers . . . . .	77
	References . . . . .	80
<b>4</b>	<b>Simulation of Piezoelectric Sensor and Actuator Devices . . . . .</b>	<b>83</b>
4.1	Basic Steps of Finite Element Method . . . . .	84
4.1.1	Finite Element Method for a One-Dimensional Problem . . . . .	85
4.1.2	Spatial Discretization and Efficient Computation . . . . .	89
4.1.3	Ansatz Functions . . . . .	91
4.1.4	Time Discretization . . . . .	94
4.2	Electrostatics . . . . .	95
4.3	Mechanical Field . . . . .	98
4.3.1	Types of Analysis . . . . .	101
4.3.2	Attenuation within Mechanical Systems . . . . .	104
4.3.3	Example . . . . .	105
4.4	Acoustic Field . . . . .	108
4.4.1	Open Domain Problems . . . . .	110
4.4.2	Example . . . . .	113
4.5	Coupled Fields . . . . .	115
4.5.1	Piezoelectricity . . . . .	115
4.5.2	Mechanical–Acoustic Coupling . . . . .	122
	References . . . . .	125
<b>5</b>	<b>Characterization of Sensor and Actuator Materials . . . . .</b>	<b>127</b>
5.1	Standard Approaches for Characterization . . . . .	128
5.1.1	IEEE/CENELEC Standard on Piezoelectricity . . . . .	128
5.1.2	Characterization Approaches for Passive Materials . . . . .	136
5.2	Fundamentals of Inverse Method . . . . .	141
5.2.1	Definition of Inverse Problems . . . . .	141
5.2.2	Inverse Method for Material Characterization . . . . .	142
5.2.3	Tikhonov Regularization . . . . .	143
5.2.4	Iteratively Regularized Gauss–Newton Method . . . . .	145
5.3	Inverse Method for Piezoceramic Materials . . . . .	147
5.3.1	Material Parameters and Modeling of Attenuation . . . . .	149
5.3.2	Feasible Input Quantities . . . . .	150

5.3.3	Test Samples . . . . .	150
5.3.4	Mathematical Procedure . . . . .	155
5.3.5	Efficient Implementation . . . . .	157
5.3.6	Results for Selected Piezoceramic Materials . . . . .	158
5.4	Inverse Method for Passive Materials . . . . .	165
5.4.1	Material Model and Modeling of Attenuation . . . . .	166
5.4.2	Feasible Input Quantities . . . . .	172
5.4.3	Test Samples . . . . .	173
5.4.4	Efficient Implementation . . . . .	180
5.4.5	Identified Parameters for Selected Materials . . . . .	184
	References . . . . .	190
<b>6</b>	<b>Phenomenological Modeling for Large-Signal Behavior of Ferroelectric Materials . . . . .</b>	<b>195</b>
6.1	Mathematical Definition of Hysteresis . . . . .	197
6.2	Modeling Approaches on Different Length Scales . . . . .	198
6.3	Phenomenological Modeling Approaches . . . . .	201
6.4	Modeling of Preisach Hysteresis Operator . . . . .	204
6.4.1	Preisach Hysteresis Model . . . . .	204
6.4.2	Efficient Numerical Calculation . . . . .	209
6.5	Weighting Procedures for Switching Operators . . . . .	213
6.5.1	Spatially Discretized Weighting Distribution . . . . .	214
6.5.2	Analytical Weighting Distribution . . . . .	218
6.6	Generalized Preisach Hysteresis Model . . . . .	224
6.6.1	Reversible Parts . . . . .	224
6.6.2	Asymmetric Behavior . . . . .	226
6.6.3	Mechanical Deformations . . . . .	228
6.6.4	Rate-Dependent Behavior . . . . .	230
6.6.5	Uniaxial Mechanical Stresses . . . . .	234
6.7	Parameter Identification for Preisach Modeling . . . . .	239
6.7.1	Identification Strategy for Model Parameters . . . . .	239
6.7.2	Application to Piezoceramic Disk . . . . .	242
6.8	Inversion of Preisach Hysteresis Model . . . . .	242
6.8.1	Inversion Procedure . . . . .	245
6.8.2	Characterization of Inversion Procedure . . . . .	249
6.8.3	Inverting Generalized Preisach Hysteresis Model . . . . .	252
6.8.4	Hysteresis Compensation for Piezoceramic Disk . . . . .	252
	References . . . . .	254
<b>7</b>	<b>Piezoelectric Ultrasonic Transducers . . . . .</b>	<b>261</b>
7.1	Calculation of Sound Fields and Electrical Transducer Outputs . . . . .	262
7.1.1	Diffraction at Point-Like Target . . . . .	263
7.1.2	Spatial Impulse Response (SIR) . . . . .	265

- 7.1.3 SIR of Piston-Type Transducer . . . . . 267
- 7.1.4 SIR of Spherically Focused Transducer . . . . . 269
- 7.2 Sound Fields and Directional Characteristics . . . . . 272
  - 7.2.1 Piston-Type Transducer . . . . . 274
  - 7.2.2 Spherically Focused Transducer . . . . . 281
- 7.3 Spatial Resolution in Pulse-Echo Mode . . . . . 289
  - 7.3.1 Transducer Excitation and Resulting Output . . . . . 289
  - 7.3.2 Axial Resolution . . . . . 291
  - 7.3.3 Lateral Resolution . . . . . 292
- 7.4 General Structure . . . . . 295
  - 7.4.1 Single-Element Transducers . . . . . 296
  - 7.4.2 Transducer Arrays . . . . . 301
  - 7.4.3 Piezoelectric Composite Transducers . . . . . 306
- 7.5 Analytical Modeling . . . . . 308
  - 7.5.1 Equivalent Electrical Circuits . . . . . 311
  - 7.5.2 Calculation Procedure . . . . . 312
  - 7.5.3 Exemplary Results . . . . . 316
- 7.6 Examples for Piezoelectric Ultrasonic Transducers . . . . . 319
  - 7.6.1 Airborne Ultrasound . . . . . 319
  - 7.6.2 Underwater Ultrasound . . . . . 324
  - 7.6.3 Medical Diagnostics . . . . . 330
- 7.7 Ultrasonic Imaging . . . . . 331
  - 7.7.1 A-Mode and M-Mode Imaging . . . . . 332
  - 7.7.2 B-Mode Imaging . . . . . 333
  - 7.7.3 C-Mode Imaging . . . . . 334
- References . . . . . 336

- 8 Characterization of Sound Fields Generated by Ultrasonic Transducers . . . . . 341**
  - 8.1 Conventional Measurement Principles . . . . . 341
    - 8.1.1 Hydrophones . . . . . 342
    - 8.1.2 Microphones . . . . . 343
    - 8.1.3 Pellicle-Based Optical Interferometry . . . . . 345
    - 8.1.4 Schlieren Optical Methods . . . . . 346
    - 8.1.5 Light Diffraction Tomography . . . . . 347
    - 8.1.6 Comparison . . . . . 348
  - 8.2 History of Light Refractive Tomography . . . . . 348
  - 8.3 Fundamentals of Light Refractive Tomography . . . . . 349
    - 8.3.1 Measurement Principle . . . . . 349
    - 8.3.2 Tomographic Imaging . . . . . 352
    - 8.3.3 Measurement Procedure and Realized Setup . . . . . 356
    - 8.3.4 Decisive Parameters for LRT Measurements . . . . . 358

8.3.5	Sources for Measurement Deviations . . . . .	364
8.3.6	Measurable Sound Frequency Range . . . . .	370
8.4	Sound Fields in Water . . . . .	372
8.4.1	Piston-Type Ultrasonic Transducer . . . . .	373
8.4.2	Cylindrically Focused Ultrasonic Transducer . . . . .	376
8.4.3	Acceleration of Measurement Process . . . . .	378
8.4.4	Disturbed Sound Field due to Hydrophones . . . . .	382
8.5	Sound Fields in Air . . . . .	387
8.5.1	Piezo-optic Coefficient in Air . . . . .	387
8.5.2	Experimental Setup . . . . .	388
8.5.3	Results for Piston-Type Ultrasonic Transducer . . . . .	390
8.6	Mechanical Waves in Optically Transparent Solids . . . . .	394
8.6.1	Normal Stress in Isotropic Solids . . . . .	394
8.6.2	Experimental Setup . . . . .	395
8.6.3	Results for Different Ultrasonic Transducers . . . . .	396
8.6.4	Verification of Experimental Results . . . . .	401
	References . . . . .	404
<b>9</b>	<b>Measurement of Physical Quantities and Process Measurement Technology . . . . .</b>	<b>407</b>
9.1	Force, Torque, Pressure, and Acceleration . . . . .	409
9.1.1	Fundamentals . . . . .	409
9.1.2	Force and Torque . . . . .	412
9.1.3	Pressure . . . . .	415
9.1.4	Acceleration . . . . .	418
9.1.5	Readout of Piezoelectric Sensors . . . . .	422
9.2	Determination of Plate Thickness and Speed of Sound . . . . .	428
9.2.1	Measurement Principle . . . . .	429
9.2.2	Transmission Line Model for Plate . . . . .	431
9.2.3	Excitation Signal of Transmitter . . . . .	434
9.2.4	Pulse Compression . . . . .	440
9.2.5	Experiments . . . . .	446
9.3	Fluid Flow . . . . .	452
9.3.1	Fundamentals of Fluid Flow Measurements . . . . .	453
9.3.2	Measurement Principles of Ultrasonic Flow Meters . . . . .	456
9.3.3	Arrangement of Ultrasonic Transducers . . . . .	465
9.3.4	Modeling of Clamp-on Transit Time Ultrasonic Flow Meters in Frequency–Wavenumber Domain . . . . .	469
9.4	Cavitation Sensor for Ultrasonic Cleaning . . . . .	484
9.4.1	Fundamentals of Acoustic Cavitation and Ultrasonic Cleaning . . . . .	484
9.4.2	Conventional Measurements of Cavitation Activity . . . . .	492

- 9.4.3 Realized Sensor Array . . . . . 493
- 9.4.4 Characterization of Sensor Array . . . . . 495
- 9.4.5 Experimental Results . . . . . 501
- References . . . . . 505
- 10 Piezoelectric Positioning Systems and Motors . . . . . 511**
  - 10.1 Piezoelectric Stack Actuators . . . . . 512
    - 10.1.1 Fundamentals . . . . . 512
    - 10.1.2 Effect of Mechanical Prestress on Stack Performance . . . . . 516
    - 10.1.3 Preisach Hysteresis Modeling for Prestressed Stack . . . 518
  - 10.2 Amplified Piezoelectric Actuators . . . . . 521
    - 10.2.1 Working Principle . . . . . 522
    - 10.2.2 Numerical Simulations for Parameter Studies . . . . . 523
    - 10.2.3 Experimental Verification . . . . . 528
  - 10.3 Piezoelectric Trimorph Actuators . . . . . 531
    - 10.3.1 Preisach Hysteresis Modeling for Trimorph . . . . . 531
    - 10.3.2 Model-Based Hysteresis Compensation for Trimorph . . . . . 533
  - 10.4 Piezoelectric Motors . . . . . 538
    - 10.4.1 Linear Piezoelectric Motors . . . . . 539
    - 10.4.2 Rotary Piezoelectric Motors . . . . . 544
  - References . . . . . 548
- Index . . . . . 551**

# Chapter 1

## Introduction



Piezoelectric devices play a major role in our everyday lives. Currently, the global demand for piezoelectric devices is valued at approximately 20 billion euros per year. Piezoelectric sensors and actuators make a substantial contribution in this respect. At the beginning of the opening chapter, we will discuss the fundamentals of sensors and actuators. Section 1.2 addresses the history of piezoelectricity and piezoelectric materials. In Sect. 1.3, application areas as well as application examples of piezoelectricity are listed. The chapter ends with a brief chapter overview of the book.

### 1.1 Fundamentals of Sensors and Actuators

Sensors and actuators play an important role in various practical applications. Let us start with the fundamentals of sensors. In general, sensors convert measurands into appropriate measurement values. From the system point of view, measurands serve as inputs and measurement values as outputs of sensors. In this book, sensors will be limited to devices that convert mechanical quantities into electrical quantities. The mechanical quantities denote, thus, measurands, while the electrical quantities represent measurement values. Figure 1.1 depicts possible measurands (e.g., mechanical force) and measurement values (e.g., electric voltage).

In contrast to sensors, (electromechanical) actuators convert electrical quantities (e.g., electric voltage) into mechanical quantities (e.g., mechanical force). Hence, actuators operate in opposite direction as sensors (see Fig. 1.1). From the system point of view, electrical quantities serve as inputs, whereas mechanical quantities represent outputs of actuators.

There exist several principles to convert mechanical into electrical quantities and electrical into mechanical quantities. Some conversion principles work in both directions, i.e., it is possible to convert mechanical into electrical quantities and vice versa. Due to this fact, such conversion principles can be exploited for sensors and actuators.

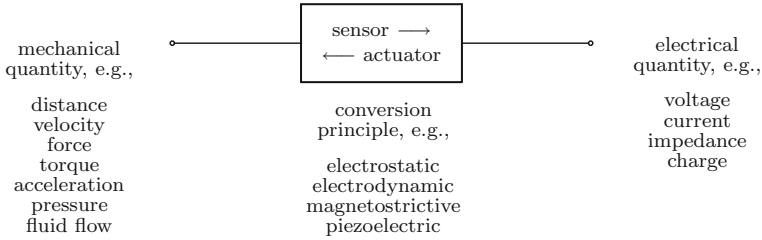


**Fig. 1.1** Typical conversion principles as well as input and output quantities of sensors and actuators

ators. The most common bidirectional conversion principles are listed in Fig. 1.1. If a conversion principle allows both working directions, sensors and actuators will often be called *transducers*. As the book title implies, we will focus on the piezoelectric conversion principle. Therefore, the book deals with piezoelectric sensors and piezoelectric actuators, i.e., with piezoelectric transducers.

Apart from the conversion principle, sensors and actuators can be classified according to other aspects. Especially for sensors, one can find several classifications like active/passive sensors. Because piezoelectric sensors do not necessarily need an auxiliary energy, they belong to the group of active sensors.

## 1.2 History of Piezoelectricity and Piezoelectric Materials

The word *piezoelectricity* originates from the Greek language and means electricity due to pressure. Piezoelectricity was firstly discovered by the Curie brothers in 1880. They recognized that electric charges will arise when mechanical forces are applied to materials like tourmaline, quartz, topaz, and Rochelle salt. This effect is referred to as *direct piezoelectric effect*. In 1881, Lippmann deduced the *inverse piezoelectric effect* from the mathematical point of view. The Curie brothers immediately confirmed the existence of the inverse piezoelectric effect.

The first practical application of piezoelectricity was the sonar, which has been developed during the First World War by Langevin. The main component of the sonar consisted of a thin quartz crystal that was glued between two steel plates. In 1921, Cady invented an electrical oscillator, which was stabilized by a quartz crystal. A few years later, such oscillators were used in all high-frequency radio transmitters. Quartz crystal controlled oscillators are nowadays still the secondary standard for timing and frequency control. The success of sonar and quartz crystal controlled oscillators was responsible that new piezoelectric materials and new applications were explored over the next decades after the First World War. For example, the development of piezoelectric ultrasonic transducers enabled viscosity measurements in fluids and the detection of flaws inside of solids.

During the Second World War, several independent research groups discovered a new class of synthetic materials, which offers piezoelectric constants many times higher than natural materials such as quartz. The synthetically produced polycrys-

talline ceramic materials were named ferroelectrics and piezoceramic materials. Barium titanate and lead zirconate titanate (PZT) represent two well-known solid solutions that belong to the class of these materials. In 1946, it was demonstrated that barium titanate features pronounced piezoelectric properties after an appropriate poling process. The first commercial use of barium titanate was in phonograph pick-ups. The strong piezoelectric coupling in PZT was discovered in 1954. The intense research in the following decades revealed that the piezoelectric properties of PZT could be controlled by means of doping. In doing so, it is possible to produce ferroelectrically soft and ferroelectrically hard materials. While ferroelectrically soft materials are well suited for piezoelectric actuators and ultrasonic transducers, ferroelectrically hard materials provide an outstanding stability for high power and filter applications. On these grounds, PZT is most commonly used in conventional piezoelectric devices, nowadays.

Even though piezoceramic materials such as PZT feature comparatively high electromechanical coupling factors and can be manufactured in arbitrary shape, quartz crystals still play an important role in practical applications, e.g., for piezoelectric force sensors. There are several reasons for this. For instance, special cuts of quartz crystals lead to material properties that are stable over a wide temperature range as well as almost free of hysteresis. Moreover, quartz crystals can also be synthetically manufactured by the so-called hydrothermal method, which was firstly applied to artificially grow quartz in the 1940s. Aside from quartz, lithium niobate and lithium tantalate are well-known representatives of piezoelectric single crystals. Both materials play a key role in modern telecommunication systems because they often serve as piezoelectric material for surface acoustic wave (SAW) devices.

Over the past decades, the research in the field of piezoelectric materials has concentrated on various topics. Many research groups work on lead-free piezoceramic materials (e.g., sodium potassium niobate) that provide a similar performance as PZT. A further research topic concerns relaxor-based single crystals since the piezoelectric constants of such piezoelectric materials can take values, which greatly exceed those of PZT. Because microelectromechanical systems (MEMS) gain in importance, much research and development are also conducted in the fabrication of thick and thin piezoelectric films. As a last example of research topics, let us mention piezoelectric polymers like polyvinylidene fluoride (PVDF) and cellular polypropylene. If the piezoelectric polymers are produced as thin films, they can be exploited for mechanically flexible sensors and actuators.

### 1.3 Practical Applications of Piezoelectricity

The application areas of piezoelectricity range from process measurement technology, nondestructive testing and medicine to consumer electronics and sports. Depending on the particular application, one exploits the direct piezoelectric effect, the inverse piezoelectric effect or a combination of both. The following list contains selected applications (e.g., parking sensors) in different application areas.

- process measurement technology and condition monitoring
  - sensors for, e.g., force, torque, acceleration, viscosity
  - measurement of temperature and geometric distance
- automotive industry
  - parking sensors
  - injection systems in diesel engines
- production technology
  - ultrasonic welding
  - ultrasonic cleaning
- nondestructive testing
  - flaw detection
  - material and device characterization
- medicine
  - diagnostics, e.g., pregnancy examinations
  - therapy, e.g., kidney stone fragmentation (lithotripsy)
- consumer electronics
  - loudspeakers
  - inkjet printers
  - lens settings in cameras
- smart materials and structures
  - active noise control
  - structural health monitoring
- sports, e.g., reduction of mechanical vibrations in tennis rackets
- musics, e.g., pickup for guitars
- energy harvesting for local energy supply
- transformers

Even though this list of applications seems to be very long, it could be extended almost indefinitely.

## 1.4 Chapter Overview

As the title suggests, the book deals with fundamentals and applications of piezoelectric sensors and actuators. According to the list in the previous section, there exists a wide variety of applications of piezoelectricity. In this book, we will concentrate on some selected examples. Many topics refer to research activities, which have

been conducted at the Chair of Sensor Technology (Friedrich-Alexander-University Erlangen-Nuremberg) during the last ten years. Apart from the opening chapter, the book is divided into nine chapters.

Chapter 2 addresses the physical basics that are important for piezoelectric sensors and actuators. This includes fundamentals, characteristic quantities as well as basic equations of electromagnetics, continuum mechanics, and acoustics. In Chap. 3, we will study the fundamentals of piezoelectricity. The chapter starts with the principle of the direct and inverse piezoelectric effect. After thermodynamical considerations, the material law of linear piezoelectricity will be derived. Furthermore, the electromechanical coupling inside piezoelectric materials will be classified and quantitatively rated. The chapter ends with a comprehensive overview of piezoelectric materials (e.g., polycrystalline ceramic materials), which are used in practical applications.

Chapter 4 deals with the fundamentals of finite element (FE) simulations since such numerical simulations are nowadays the standard tool for the design and optimization of piezoelectric sensors and actuators. We will start with the basic steps of the FE method. Afterward, the FE method will be applied to the electrostatic field, the mechanical field, and the acoustic field. Due to the fact that piezoelectricity refers to coupling of mechanical and electric quantities, we study the simulation-based coupling of the underlying fields. This also includes the coupling of mechanical and acoustic fields, which is important for piezoelectric ultrasonic transducers.

In Chap. 5, we will discuss the characterization of sensor and actuator materials. The material characterization represents an essential step in the design and optimization because reliable numerical simulations demand precise material parameters. The chapter starts with standard approaches for material characterization. In doing so, a clear distinction between active and passive materials is carried out. Piezoelectric materials are active materials, whereas other materials (e.g., plastics) within piezoelectric sensors and actuators belong to the group of passive materials. The main focus of the chapter lies on the so-called inverse method, which has been developed at the Chair of Sensor Technology. Basically, the inverse method combines FE simulations with measurements. By reducing the deviations between simulation and measurement results, the material parameters get iteratively adjusted in a convenient way. The inverse method is exploited to identify material parameters and properties of selected active and passive materials.

Piezoceramic materials will show a pronounced hysteretic behavior if large electrical excitation signals are used during operation. Chapter 6 details a phenomenological modeling approach, which allows the reliable description of this large-signal behavior. Before the so-called Preisach hysteresis operator is introduced, we will briefly study various modeling approaches on different length scales. Since the Preisach hysteresis operator consists of weighted elementary switching operators, two different weighting procedures are given. The chapter also addressed generalized Preisach hysteresis models, which have been developed at the Chair of Sensor Technology. For instance, the generalization enables the consideration of mechanical stresses that are applied to a piezoceramic material. Finally, we discuss the inversion of the Preisach hysteresis model. The inversion will be of utmost importance when the Preisach hysteresis operator is used for hysteresis compensation.

Chapter 7 treats ultrasonic transducers that exploit piezoelectric materials. The chapter starts with a semi-analytical approach for calculating sound fields and transducer outputs. The approach is based on the so-called spatial impulse response (SIR) of the considered ultrasonic transducer, e.g., a piston-type transducer. Among other things, the SIR is utilized to determine the spatial resolution of spherically focused transducers. Afterward, we will study the general structure and fundamental operation modes of single-element transducers, transducer arrays, and composite transducers. A further section concerns a simple one-dimensional modeling approach that allows analytical description of basic physical relations under consideration of the internal transducer structure. At the end of the chapter, several examples for piezoelectric ultrasonic transducers will be presented.

Practical applications of ultrasonic transducers often demand the characterization of the resulting sound fields. That is the reason why Chap. 8 deals with appropriate measurement principles. The chapter starts with conventional measurement principles such as hydrophones and Schlieren optical methods. The subsequent sections exclusively concentrate on the so-called light refractive tomography (abbr. LRT), which has been realized at the Chair of Sensor Technology. This optical measurement principle enables nonreactive and spatially as well as temporally resolved investigations of sound fields that are generated by piezoelectric ultrasonic transducers, e.g., a cylindrically focused transducer. Exemplary results for sound pressure fields in water and air will be shown. Moreover, LRT is applied to study the wave propagation of mechanical waves in an optically transparent solid.

Piezoelectric sensors are frequently employed for the measurement of physical quantities. In Chap. 9, we will study typical setups of such sensors and their application in the process measurement technology. At the beginning, piezoelectric sensors for the quantities force, torque, pressure, and acceleration are detailed. This includes commonly used readout electronics such as charge amplifiers. Subsequently, a method will be presented which enables the simultaneous determination of thickness and speed of sound for solid plates. The underlying measurement principle is based on ultrasonic waves and has been developed at the Chair of Sensor Technology. The chapter also addresses fluid flow measurements that exploit ultrasonic transducers. We will discuss typical measurement principles as well as a recently suggested modeling approach, which allows efficient estimation of transducer outputs for clamp-on ultrasonic flow meters. At the end, a mechanically flexible cavitation sensor is presented that has been developed at the Chair of Sensor Technology.

The last chapter addresses piezoelectric positioning systems and piezoelectric motors. We will start with piezoelectric stack actuators, which provide much larger strokes than piezoelectric single elements. Because the large strokes call for large electrical excitation signals, Preisach hysteresis modeling from Chap. 6 is applied for a mechanically prestressed stack actuator. The subsequent section details an amplified piezoelectric actuator that was built up at the Chair of Sensor Technology. We will also study model-based hysteresis compensation for a piezoelectric trimorph actuator, which can be used for positioning tasks. The end of the chapter concerns linear and rotary piezoelectric motors.

# Chapter 2

## Physical Basics



Piezoelectric sensors and actuators connect different physical fields (e.g., electrostatic and mechanical field). With a view to studying the behavior of piezoelectric devices, the fundamentals of those physical fields are indispensable. Therefore, this chapter addresses the physical principles that are important for piezoelectric sensors and actuators. Section 2.1 deals with electromagnetics, especially with the electric field. In Sects. 2.2 and 2.3, the basics of continuum mechanics and acoustics are described, respectively.

### 2.1 Electromagnetics

In this section, the so-called Maxwell's equations as well as the relevant constitutive equations are introduced allowing the complete description of electromagnetic fields. We will discuss the electrostatic field, which represents a special case of electromagnetic fields. Section 2.1.3 details interface conditions for the electric field between two media exhibiting different material properties. Finally, the lumped circuit element approach is explained that can be exploited to efficiently solve electromagnetic field problems. Further literature concerning the electromagnetic field can be found in [1, 8, 9, 17].

#### 2.1.1 Maxwell's Equations

James Clerk Maxwell published for the first time the full system of partial differential equations, which describe the physical relations in the electromagnetic field [13, 14]. His work relies on previous research performed by Ampère, Gauss, and Faraday. The

**Table 2.1** Expressions utilized in Maxwell's equations (2.1)–(2.4)

Notation	Description	Unit
<b>H</b>	Magnetic field intensity; vector	$\text{A m}^{-1}$
<b>E</b>	Electric field intensity; vector	$\text{V m}^{-1}$
<b>B</b>	Magnetic flux density (magnetic induction); vector	$\text{V s m}^{-2}$ ; T
<b>D</b>	Electric flux density (electric induction); vector	$\text{A s m}^{-2}$ ; $\text{C m}^{-2}$
$q_e$	Volume charge density; scalar	$\text{A s m}^{-3}$ ; $\text{C m}^{-3}$
<b>J</b>	Electric current density; vector	$\text{A m}^{-2}$
<b>M</b>	Magnetization; vector	$\text{V s m}^{-2}$ ; T
<b>P</b>	Electric polarization; vector	$\text{A s m}^{-2}$ ; $\text{C m}^{-2}$

four Maxwell's equations<sup>1</sup> in differential form are given by (time  $t$ ; Nabla operator  $\nabla = [\partial/\partial x, \partial/\partial y, \partial/\partial z]^t$ )

$$\text{Law of Ampère: } \nabla \times \mathbf{H} = \mathbf{J} + \frac{\partial \mathbf{D}}{\partial t} \quad (2.1)$$

$$\text{Law of Faraday: } \nabla \times \mathbf{E} = -\frac{\partial \mathbf{B}}{\partial t} \quad (2.2)$$

$$\text{Law of Gauss: } \nabla \cdot \mathbf{D} = q_e \quad (2.3)$$

$$\nabla \cdot \mathbf{B} = 0 \quad (2.4)$$

with the expressions listed in Table 2.1. The general form of Maxwell's equations contains the displacement current ( $\partial \mathbf{D}/\partial t$ ) in (2.1) and is, therefore, also applicable in the high-frequency domain of electromagnetic fields. However, for the low-frequency domain (quasi-static case), the wavelength  $\lambda$  of the resulting electromagnetic waves is large compared to the dimensions of conventional electromagnetic devices. That is the reason why (2.1) can be simplified to  $\nabla \times \mathbf{H} = \mathbf{J}$ .

Several properties of electromagnetic fields can be deduced from Maxwell's equations. The most important findings are listed below.

- Law of Ampère: An electric current density  $\mathbf{J}$  generates a magnetic field. The directions of the magnetic field lines relate to the direction of  $\mathbf{J}$  according to the so-called right-hand rule (see Fig. 2.1a).
- Law of Faraday: A magnetic flux density  $\mathbf{B}$  that is changing with respect to time induces an electric voltage in a conductive loop (see Fig. 2.1b).
- Law of Gauss: Electric charges are the source of the electric field (see Fig. 2.1c).
- Fourth Maxwell's equation: The magnetic field ( $\mathbf{B}$ ,  $\mathbf{H}$ ) is solenoidal and, therefore, the magnetic field lines are closed (see Fig. 2.1d). Furthermore, magnetic charges do not exist.

<sup>1</sup>To achieve a compact form of the subsequent equations, the arguments for both position  $\mathbf{r}$  and time  $t$  (i.e.,  $\bullet(\mathbf{r}, t)$ ) are mostly omitted. Note that this is also done for continuum mechanics as well as for acoustics.

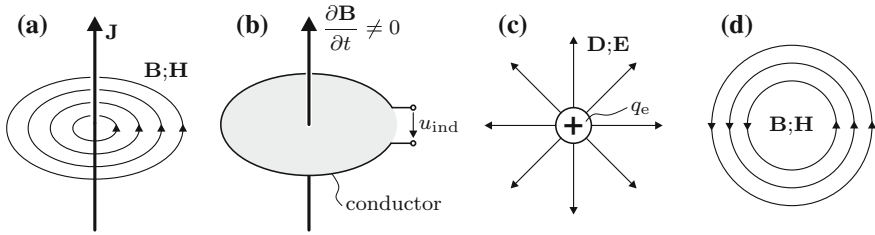


**Fig. 2.1** Basic interpretations for **a** Law of Ampère, **b** Law of Faraday (induced electrical voltage  $u_{\text{ind}}$ ), **c** Law of Gauss ( $q_e > 0$ ), **d** fourth Maxwell's equation

**Table 2.2** Expressions utilized in constitutive equations (2.5)–(2.7)

Notation	Description	Unit
$\gamma$	Electric conductivity; scalar	$\Omega^{-1} \text{m}^{-1}$
$\mathbf{v}$	Velocity of the volume charges $q_e$ ; vector	$\text{m s}^{-1}$
$\mu$	Magnetic permeability; scalar	$\text{V s A}^{-1} \text{m}^{-1}$
$\mu_0$	Magnetic permeability of vacuum ( $4\pi \cdot 10^{-7}$ ); scalar	$\text{V s A}^{-1} \text{m}^{-1}$
$\mu_r$	Relative magnetic permeability; scalar	–
$\varepsilon$	Electric permittivity; scalar	$\text{A s V}^{-1} \text{m}^{-1}$
$\varepsilon_0$	Electric permittivity of vacuum ( $8.854 \cdot 10^{-12}$ ); scalar	$\text{A s V}^{-1} \text{m}^{-1}$
$\varepsilon_r$	Relative electric permittivity; scalar	–

In addition to Maxwell's equations, the modeling of media in the electromagnetic field requires constitutive equations, which cover the materials' behavior. For a homogeneous and isotropic material, the constitutive equations read as

$$\mathbf{J} = \gamma(\mathbf{E} + \mathbf{v} \times \mathbf{B}) \quad (2.5)$$

$$\mathbf{B} = \mu\mathbf{H} = \mu_0\mathbf{H} + \mathbf{M} = \mu_0\mu_r\mathbf{H} \quad (2.6)$$

$$\mathbf{D} = \varepsilon\mathbf{E} = \varepsilon_0\mathbf{E} + \mathbf{P} = \varepsilon_0\varepsilon_r\mathbf{E} \quad (2.7)$$

with the expressions listed in Table 2.2. Note that for anisotropic materials, such as piezoceramics, the electric and magnetic material properties (e.g.,  $\varepsilon$ ) cannot be completely assigned by single scalar quantities but demand tensors of rank  $\geq 2$ . Table 2.3 contains the electric conductivity  $\gamma$ , the relative magnetic permeability  $\mu_r$  as well as the relative electric permittivity  $\varepsilon_r$  of selected media.

### 2.1.2 Electrostatic Field

In the static case, both electric and magnetic quantities do not depend on time. Electric charges do not move and energy is neither transported nor converted. As a result,

**Table 2.3** Electric conductivity  $\gamma$ , relative magnetic permeability  $\mu_r$ , and relative electric permittivity  $\varepsilon_r$  of selected media

Media	$\gamma$ in $\Omega^{-1} \text{ m}^{-1}$	$\mu_r$	$\varepsilon_r$
Copper	$59 \cdot 10^6$	1	–
Iron	$10 \cdot 10^6$	>300	–
Tungsten	$18 \cdot 10^6$	1	–
PVDF*	$10^{-11}$	1	6
Polyethylene	$10^{-13}$	1	2.4
Water	$5 \cdot 10^{-3}$	1	80

\* Polyvinylidene fluoride

Maxwell's equations and the constitutive equations can be divided into an electric and a magnetic subsystem. For the so-called electrostatic field (electric subsystem), the relations between the electric quantities can be described with

$$\nabla \times \mathbf{E} = 0 \quad (2.8)$$

$$\nabla \cdot \mathbf{D} = q_e \quad (2.9)$$

$$\mathbf{D} = \varepsilon \mathbf{E} . \quad (2.10)$$

Since the electric field intensity  $\mathbf{E}$  is irrotational (see (2.8)), it can be expressed by the so-called electric scalar potential  $V_e$

$$\mathbf{E} = -\nabla V_e . \quad (2.11)$$

Note that (2.8)–(2.11) will also be appropriate for quasi-static electric fields if the resulting magnetic quantities are still negligible. This is the case for materials exhibiting small relative magnetic permeabilities  $\mu_r$ .

### 2.1.3 Interface Conditions for Electric Field

At an interface of different media, the quantities of electric and/or magnetic fields may be altered. To study this for the electric field, we assume an interface between two isotropic homogeneous materials showing different electric permittivities ( $\varepsilon_1$  and  $\varepsilon_2$ ; Fig. 2.2a). The starting point to derive the interface conditions is Maxwell's equations. The third Maxwell's equation (Law of Gauss; (2.3)) in integral form is given as (volume  $\Omega$ , surface  $\Gamma$ , surface vector  $\mathbf{\Gamma}$ )

$$\int_{\Omega} (\nabla \cdot \mathbf{D}) \, d\Omega = \oint_{\Gamma} \mathbf{D} \cdot d\mathbf{\Gamma} = \int_{\Omega} q_e \, d\Omega \quad (2.12)$$

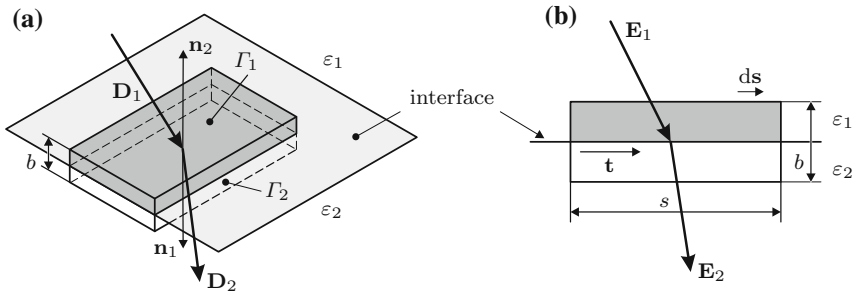


**Fig. 2.2** Interface of different media: **a** continuity of electric flux density  $\mathbf{D}$ ; **b** continuity of electric field intensity  $\mathbf{E}$

where the divergence theorem has been applied. Using the relation  $d\Omega = b d\Gamma$  and the assumption  $b \rightarrow 0$  results in

$$\lim_{b \rightarrow 0} \int_{\Omega} q_e d\Omega = \int_{\Gamma} \sigma_e d\Gamma . \quad (2.13)$$

Here,  $\sigma_e$  denotes the surface charge. Furthermore, (2.12) can be rewritten to

$$\lim_{b \rightarrow 0} \oint_{\Gamma} \mathbf{D} \cdot d\Gamma \longrightarrow \mathbf{D}_1 \cdot \mathbf{n}_1 + \mathbf{D}_2 \cdot \mathbf{n}_2 = \mathbf{n}_1 (\mathbf{D}_1 - \mathbf{D}_2) = D_{1n} - D_{2n} \quad (2.14)$$

with the normal vectors  $\mathbf{n}_1$  and  $\mathbf{n}_2$  at the material interface. The expressions  $D_{1n}$  and  $D_{2n}$  indicate the normal components of  $\mathbf{D}_1$  and  $\mathbf{D}_2$ , respectively. The combination of (2.13) and (2.14) yields the continuity relation for the electric flux density  $\mathbf{D} = [D_n, D_t]^t$

$$D_{1n} = D_{2n} + \sigma_e . \quad (2.15)$$

Assuming a negligible magnetic field, the second Maxwell's equation (Law of Faraday; (2.2)) in integral form becomes (closed contour  $\mathcal{C}$ )

$$\int_{\mathcal{C}} (\nabla \times \mathbf{E}) \cdot d\Gamma = \oint_{\mathcal{C}} \mathbf{E} \cdot ds = 0 \quad (2.16)$$

where Stoke's theorem has been applied. For the material interface shown in Fig. 2.2b and  $b \rightarrow 0$ , we can simplify (2.16) to

$$\lim_{b \rightarrow 0} \oint_{\mathcal{C}} \mathbf{E} \cdot ds \longrightarrow \mathbf{E}_1 \cdot \mathbf{s} - \mathbf{E}_2 \cdot \mathbf{s} = \mathbf{s}t \cdot (\mathbf{E}_1 - \mathbf{E}_2) = E_{1t} - E_{2t} = 0 . \quad (2.17)$$

Consequently, the tangential component  $E_t$  of the electric field intensity  $\mathbf{E} = [E_n, E_t]^t$  is continuous at the interface of two materials.

By performing similar steps, the continuity relations at a material interface for the magnetic quantities ( $\mathbf{B}$ ,  $\mathbf{H}$ ) and for the electric current density  $\mathbf{J}$  can be deduced.

### 2.1.4 Lumped Circuit Elements

As previously discussed, we will be able to simplify Maxwell's equations when the device dimensions are much smaller than the wavelength of electromagnetic waves. A further simplification can be performed if either the electric or the magnetic field dominates. The application of the resulting equations is, however, oftentimes still too complicated for various practical situations. Therefore, an alternative approach is commonly utilized yielding reliable approximations of electromagnetic fields. The approach is based on three lumped circuit elements<sup>2</sup>: (i) resistor  $R$ , (ii) inductor  $L$ , and (iii) capacitor  $C$  (graphic symbols in Table 2.4) [1]. While the inductor relates to the magnetic field, the capacitor belongs to the electric field. The inductor and capacitor measure the ability to store magnetic energy and electric charges, respectively. By means of the resistor, we can describe conversions of electromagnetic energy into energy in other physical fields, e.g., kinetic energy in the mechanical field.

The relation between the physical field quantities ( $\mathbf{E}$ ;  $\mathbf{D}$ ;  $\mathbf{B}$ ;  $\mathbf{J}$ ) of electromagnetic fields and the lumped circuit elements ( $R$ ;  $L$ ;  $C$ ) is defined as

$$R = \frac{\int_{r_1}^{r_2} \mathbf{E} \cdot d\mathbf{s}}{\int_A \mathbf{J} \cdot d\mathbf{A}} = \frac{U}{I} \quad \text{unit } \Omega \quad (2.18)$$

$$L = \frac{\int_A \mathbf{B} \cdot d\mathbf{A}}{\int_A \mathbf{J} \cdot d\mathbf{A}} = \frac{\Phi}{I} \quad \text{unit H} \quad (2.19)$$

$$C = \frac{\oint_S \mathbf{D} \cdot d\mathbf{A}}{\int_{r_1}^{r_2} \mathbf{E} \cdot d\mathbf{s}} = \frac{Q}{U} \quad \text{unit F} . \quad (2.20)$$

Here,  $U$ ,  $I$ ,  $\Phi$  as well as  $Q$  stand for scalar quantities that are frequently applied in conjunction with lumped circuit elements in electrical engineering. The electric current  $I = \int_A \mathbf{J} \cdot d\mathbf{A}$  (unit A) relates to electric charges flowing through the area  $A$ . The expression  $U = \int_{r_1}^{r_2} \mathbf{E} \cdot d\mathbf{s}$  (unit V) denotes the electric potential difference (electric voltage) from position  $\mathbf{r}_2$  and  $\mathbf{r}_1$ .  $\Phi = \int_A \mathbf{B} \cdot d\mathbf{A}$  (unit Vs) is the magnetic flux through the area  $A$  and  $Q = \oint_S \mathbf{D} \cdot d\mathbf{A}$  (unit As) the electric charge enclosed by the

<sup>2</sup>Usually, these lumped circuit elements are time-invariant. Exceptions are configurations changing their geometry with respect to time.

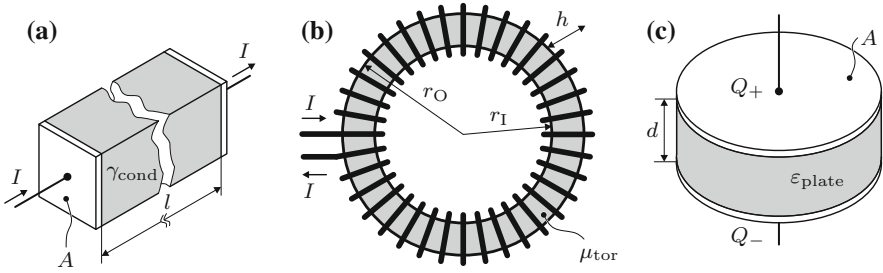


**Fig. 2.3** **a** Electric conductor (length  $l$ ; area  $A$ ) with homogeneous conductivity  $\gamma_{\text{cond}}$ ; **b** toroidal core coil (number of winding  $N_{\text{wind}}$ ; inner radius  $r_I$ ; outer radius  $r_O$ ; height  $h$ ) with relative magnetic permeability  $\mu_{\text{tor}}$ ; **c** plate capacitor (plate distance  $d$ ; area  $A$ ) containing dielectric medium with relative permittivity  $\varepsilon_{\text{plate}}$

surface  $\mathcal{S}$ . Equation (2.18) represents the so-called *Ohm's law*, which is one of the most famous equations in electrical engineering.

For simple configurations such as a conductor, a toroidal core coil (number of windings  $N_{\text{wind}}$ ), and a plate capacitor (see Fig. 2.3), we can approximate the lumped circuit elements with

$$\text{conductor:} \quad R_{\text{cond}} = \frac{l}{\gamma_{\text{cond}} A} \quad (2.21)$$

$$\text{toroidal core coil:} \quad L_{\text{tor}} = N_{\text{wind}}^2 \frac{\mu_0 \mu_{\text{tor}} h}{2\pi} \ln\left(\frac{r_O}{r_I}\right) \quad (2.22)$$

$$\text{plate capacitor:} \quad C_{\text{plate}} = \frac{\varepsilon_{\text{plate}} \varepsilon_0 A}{d} . \quad (2.23)$$

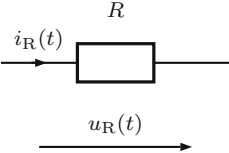
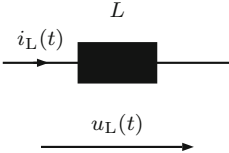
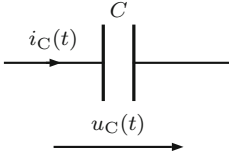
The expressions  $l$ ,  $A$ ,  $h$ ,  $r_O$ ,  $r_I$ , and  $d$  are geometric dimensions of the components.  $\gamma_{\text{cond}}$ ,  $\mu_{\text{tor}}$ , and  $\varepsilon_{\text{plate}}$  refer to the decisive material properties. For several configurations of complex geometries, similar approximations can be found.

In contrast to the simplified Maxwell's equations describing purely electric or purely magnetic fields, the lumped elements approach is also applicable in case of spatially separated components of these fields, e.g., a coil in combination with a capacitor. To efficiently investigate the behavior of such combinations with respect to time, an electric circuit containing the lumped elements and sources of electric energy (voltage source and/or current source) is analyzed. For such electric circuits, Kirchhoff's current law and Kirchhoff's voltage law have to be fulfilled at any time

$$\text{Kirchhoff's current law:} \quad \sum_{k=1}^n I_k = 0 \quad (2.24)$$

$$\text{Kirchhoff's voltage law:} \quad \sum_{k=1}^n U_k = 0 . \quad (2.25)$$

**Table 2.4** Fundamental relations and common graphic symbols for lumped elements resistor  $R$ , inductor  $L$ , and capacitor  $C$

resistor	inductor	capacitor
		
$u_x(t) = f(i_x(t), x)$ for $x \in \{R; L; C\}$ :		
$i_R(t) \cdot R$	$L \frac{di_L(t)}{dt}$	$\frac{1}{C} \int_{t_0}^t i_C(t) dt + u_C(t_0)$
$i_x(t) = f(u_x(t), x)$ for $x \in \{R; L; C\}$ :		
$\frac{u_R(t)}{R}$	$\frac{1}{L} \int_{t_0}^t u_L(t) dt + i_L(t_0)$	$C \frac{du_C(t)}{dt}$
complex impedance $\underline{X}_x(\omega)$ of $x \in \{R; L; C\}$ : (imaginary unit $j = \sqrt{-1}$ ; angular frequency $\omega = 2\pi f$ )		
$\underline{X}_R = R$	$\underline{X}_L(\omega) = j\omega L$	$\underline{X}_C(\omega) = \frac{1}{j\omega C}$
impedance $X_x(s)$ of $x \in \{R; L; C\}$ in the Laplace domain (complex frequency variable $s = \sigma + j\omega$ )		
$X_R(s) = R$	$X_L(s) = sL$	$X_C(s) = \frac{1}{sC}$

Kirchhoff’s current law states that at any node of an electric circuit, the sum of the electric currents flowing into the node is equal to the sum of electric currents flowing out of the node. Kirchhoff’s voltage law states that the directed sum of the electric voltages  $U_k$  around any closed network is zero.

The relation between the time-dependent quantities electric voltage  $u(t)$  and electric current  $i(t)$  also plays a crucial role in performing circuit analysis. Table 2.4 contains these relations for the different lumped elements. In addition to differential and integral equations in the time domain, the complex impedances  $\underline{X}_x(\omega)$  of the lumped circuit elements in the frequency domain as well as those  $X_x(s)$  in the Laplace domain are listed. Complex impedances in the frequency domain facilitate the analysis of electric circuits for sinusoidal excitations of frequency  $f = \omega/2\pi$ , while the approach based on the Laplace domain can also be utilized for certain transient excitation signals [11]. In doing so, the excitation signals have to be transformed into the

frequency domain or Laplace domain, respectively. When the (complex) impedances of the components are known, we will then be able to study electric circuits comprising various lumped elements with similar approaches as for resistor networks. However, to obtain electric voltages as well as electric currents with respect to time, appropriate inverse transforms are indispensable, i.e., transform from the Laplace domain to the time domain [4].

At this point, it should be mentioned that a real device cannot be described completely by means of a single lumped element. Reliable modeling requires, strictly speaking, superposition of several lumped elements. Nevertheless, in a certain frequency range, we can approximate the device behavior by a distinct combination of a few lumped elements.

## 2.2 Continuum Mechanics

Piezoelectric materials are able to convert mechanical into electrical energy and vice versa. Because the mechanical deformations in such solids are mostly rather small during operation, we can describe the mechanical field by linear relations. In this section, the fundamental equations for linear continuum mechanics as well as essential quantities (e.g., mechanical strain) for the mechanical field are detailed. Thereby, a deformable solid body (elastic body) is considered. We start with Navier's equation linking the mechanical stress to both, inner volume forces and time-dependent body displacements. The mechanical strain and the constitutive equations for a deformable solid body will be explained in Sect. 2.2.2 and in Sect. 2.2.3, respectively. At last, we discuss different elastic wave types, which might occur in solid bodies. Further literature concerning continuum mechanics can be found in [2, 3, 18, 20].

### 2.2.1 Navier's Equation

Navier's equation is a fundamental equation in continuum mechanics. In order to derive this equation, we assume a deformable solid body of arbitrary shape at rest with prescribed volume forces  $\mathbf{f}_V$  (given body force per unit of volume; unit  $\text{N m}^{-3}$ ; e.g., gravity forces) and a support at equilibrium. Hence, the sum of all mechanical forces as well as of all mechanical torques equals zero. If a small part is cut out of the deformable solid body, forces will have to be applied to the cutting planes to still guarantee equilibrium (*Euler–Cauchy stress principle*). These forces correspond to the inner forces of the deformable solid body. Due to the fact that the applied forces are distributed across the cutting planes, it is reasonable to introduce mechanical stresses, which are defined as force per unit area.

In a first step, we cut out a cubical-shaped small part with cutting planes aligned in parallel to the Cartesian coordinate system (see Fig. 2.4a). The expressions  $\mathbf{T}_x$ ,  $\mathbf{T}_y$ ,

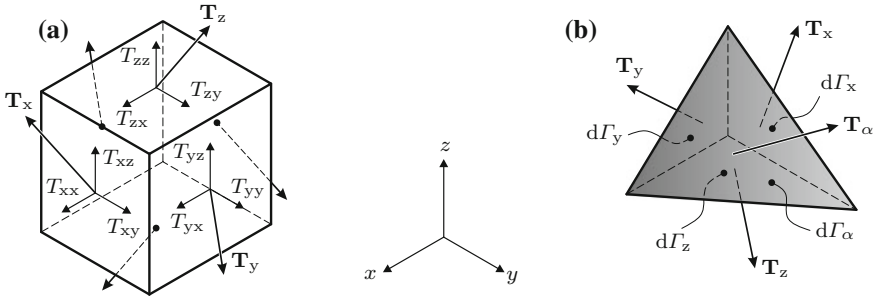


**Fig. 2.4** **a** Mechanical stresses applied to cutting planes of a cubical-shaped part of deformable solid body; **b** mechanical stresses applied to tetrahedral element exhibiting oblique surface

and  $\mathbf{T}_z$  denote the mechanical stresses (vector quantity; unit  $\text{N m}^{-2}$ ) on the cutting planes, with the index referring to the direction of their normal vector, respectively.

The stress vectors can be split up into scalar components that relate to the Cartesian coordinate system. In doing so, the stress vectors read as

$$\mathbf{T}_x = T_{xx}\mathbf{e}_x + T_{xy}\mathbf{e}_y + T_{xz}\mathbf{e}_z \quad (2.26)$$

$$\mathbf{T}_y = T_{yx}\mathbf{e}_x + T_{yy}\mathbf{e}_y + T_{yz}\mathbf{e}_z \quad (2.27)$$

$$\mathbf{T}_z = T_{zx}\mathbf{e}_x + T_{zy}\mathbf{e}_y + T_{zz}\mathbf{e}_z \quad (2.28)$$

with the unit vector  $\mathbf{e}_i$  pointing in direction  $i$ . For the scalar components  $T_{ij}$ , index  $i$  refers to normal vector's direction of the cutting plane and  $j$  stands for the direction in which the stress acts. According to this notation,  $T_{xx}$ ,  $T_{yy}$  as well as  $T_{zz}$  are normal stresses and  $T_{xy}$ ,  $T_{xz}$ ,  $T_{yx}$ ,  $T_{yz}$ ,  $T_{zx}$  as well as  $T_{zy}$  stand for shear stresses.

In a second step, we consider an infinitely small deformable body of tetrahedral shape with three surfaces ( $d\Gamma_x$ ,  $d\Gamma_y$ , and  $d\Gamma_z$ ) orientated in parallel to the Cartesian coordinate plane (see Fig. 2.4b). If a mechanical force is applied to the oblique surface  $d\Gamma_\alpha$ , the equilibrium state will require forces acting on the remaining surfaces

$$d\Gamma_x\mathbf{T}_x + d\Gamma_y\mathbf{T}_y + d\Gamma_z\mathbf{T}_z - d\Gamma_\alpha\mathbf{T}_\alpha = 0. \quad (2.29)$$

Since the unity normal vector  $\mathbf{e}_\alpha$  of the oblique surface can be defined as (Cartesian components  $n_i$ )

$$\mathbf{e}_\alpha = n_x\mathbf{e}_x + n_y\mathbf{e}_y + n_z\mathbf{e}_z, \quad (2.30)$$

the surface elements  $d\Gamma_x$ ,  $d\Gamma_y$ , and  $d\Gamma_z$  can be written as

$$d\Gamma_x = d\Gamma_\alpha n_x \quad d\Gamma_y = d\Gamma_\alpha n_y \quad d\Gamma_z = d\Gamma_\alpha n_z. \quad (2.31)$$

Combining this with (2.29) and subsequently with (2.26)–(2.28) yields

$$\begin{aligned} \mathbf{T}_\alpha &= \mathbf{T}_x n_x + \mathbf{T}_y n_y + \mathbf{T}_z n_z \\ &= (T_{xx} n_x + T_{xy} n_y + T_{xz} n_z) \mathbf{e}_x + (T_{yx} n_x + T_{yy} n_y + T_{yz} n_z) \mathbf{e}_y \\ &\quad + (T_{zx} n_x + T_{zy} n_y + T_{zz} n_z) \mathbf{e}_z . \end{aligned} \quad (2.32)$$

It is possible to achieve a compact form by exploiting the so-called *Cauchy stress tensor*  $[\mathbf{T}]$  of rank two

$$[\mathbf{T}] = \begin{bmatrix} T_{xx} & T_{xy} & T_{xz} \\ T_{yx} & T_{yy} & T_{yz} \\ T_{zx} & T_{zy} & T_{zz} \end{bmatrix} . \quad (2.33)$$

The mechanical stress acting on the oblique surface  $d\Gamma_\alpha$  of the tetrahedral can then be expressed by (transpose t)

$$\mathbf{T}_\alpha = [\mathbf{T}]^t \mathbf{e}_\alpha . \quad (2.34)$$

As already mentioned, in case of the equilibrium state, the sums of both mechanical forces and mechanical torques for the deformable solid body at rest are zero. Thus, the equation for translation (surface  $\Gamma$ ; surface vector  $\mathbf{\Gamma}$ ; volume  $\Omega$  of the body)

$$\oint_\Gamma [\mathbf{T}]^t d\mathbf{\Gamma} + \int_\Omega \mathbf{f}_V d\Omega = 0 \quad (2.35)$$

and the equation for rotation (position vector  $\mathbf{r}$  of a point in the body)

$$\oint_\Gamma (\mathbf{r} \times [\mathbf{T}]) d\mathbf{\Gamma} + \int_\Omega (\mathbf{r} \times \mathbf{f}_V) d\Omega = 0 \quad (2.36)$$

have to be fulfilled. From these two equations, it follows that the equation describing the equilibrium state for an infinitely small part of the deformable solid body at rest is given by

$$\nabla[\mathbf{T}] + \mathbf{f}_V = 0 . \quad (2.37)$$

The entries of the Cauchy stress tensor  $[\mathbf{T}]$  feature the properties

$$T_{xy} = T_{yx} \quad T_{xz} = T_{zx} \quad T_{yz} = T_{zy} . \quad (2.38)$$

Consequently,  $[\mathbf{T}]$  is symmetric and the nine tensor entries can be reduced to six entries. According to *Voigt notation*, it is convenient to introduce the stress vector  $\mathbf{T}$